Slope-weighted Energy-based Rapid Control Analysis for Hybrid Electric Vehicles

Slope-weighted Energy-based Rapid Control Analysis for Hybrid Electric Vehicles

Pier Giuseppe Anselma, *Student Member, IEEE*, Yi Huo, Joel Roeleveld, Giovanni Belingardi, Ali Emadi, *Fellow, IEEE*

***Abstract*—Recent studies have addressed the development of optimal control strategies for hybrid electric vehicles (HEVs). Achieving global optimality for the fuel economy prediction while minimizing the computational efficiency still is a research and development challenge. This paper aims at presenting a novel technique for managing the energy flows in a power split HEV named slope-weighted energy-based rapid control analysis (SERCA). After presenting the HEV plant model and the optimal control problem, the currently most adopted energy management strategies are analyzed. The SERCA technique is then illustrated and its operating steps are detailed. The simulation results for the considered HEV energy management strategies in the standard drive cycles subsequently indicate that the SERCA can efficiently achieve near-optimal fuel economy while limiting the computational costs. This suggests the potential use of SERCA for rapid component sizing of HEV powertrains.**

***Index Terms*— Control strategy, electrified powertrain, energy management, fuel consumption minimization, hybrid electric vehicles, optimal control, power split, rapid sizing**

I. Introduction

THE evolution towards a sustainable and cleaner transportation system requires higher efficiency vehicles with significantly lower fuel consumption and emissions [1]. To achieve these goals, the transportation electrification vision currently represents the leading path in society and automotive industry [2][3]. Electrical power systems provide remarkable efficiency, ease of controllability, and flexibility in the energy supply with respect to the conventional internal combustion engine (ICE) [4].

Hybrid Electric Vehicles (HEVs) are particularly registering a significant growth in popularity as they ensure improved fuel economy while satisfying customer acceptance constraints, particularly by preventing the typical range anxiety of battery electric vehicles [5]. Since its effectiveness in blending the benefits of series and parallel configurations [6], the power-split powertrain architecture reveals the most successful HEV powertrain being incorporated in the largest portion of the current population of HEVs [7]. This configuration employs the usage of planetary gear (PG) sets and performs well in many different road vehicle categories, including passenger cars [8][9][10], sport utility vehicles [11], buses [12] and heavy-duty vehicles [13].

Control strategy is considered a crucial issue in the design of HEVs. Finding an energy management strategy that guarantees optimal fuel economy, light computational burden and ease of on-board real-time implementation still represents an open research question. This paper deals with off-line HEV control strategies, where the knowledge of the vehicle speed profile for the entire considered drive cycle is needed before running the simulation. In general, off-line HEV controllers can be divided into rule-based and optimization-based procedures. Rule-based control strategies may be based on deterministic approach or fuzzy logic [14]. Typically, they guarantee reduced computational burden and ease of implementation. However, their operation can be optimized for specific drive cycles solely, therefore they rarely guarantee optimal fuel economy in various driving scenarios.

On the other hand, two main control approaches have been proposed during the past two decades related to global optimization in HEV off-line operation simulation [15]: the equivalent fuel consumption minimization Strategy (ECMS) introduced by Paganelli in 2002 [16] and based on the Pontryagin's minimum principle (PMP) [17], and dynamic programming (DP). Based on the Bellman's principle of optimality presented in 1957 [18], the DP technique was first applied in HEV studies in late 70s [19]. However, since it was constrained by the computational power needed, this approach did not draw much attention until the early 2000s. Since then, researchers and designers have been extensively studying DP and increasingly adopting it for HEV optimal control [20][21][22]. In 2008, Liu and Peng derived and applied ECMS and DP control strategies for a power-split HEV configuration [23]. In order to enable rapid component sizing of power split HEVs with multiple operating modes, Zhang et al. proposed a DP based near-optimal energy management strategy named power-weighted efficiency analysis for rapid sizing (PEARS) [24][25]. The PEARS algorithm has been studied in detail by the authors. Initially, an improved version of the algorithm minimizing mode-shifting occurrence was proposed [26]. Subsequently, the technique found application in a rapid design methodology for a multimode power split

P.G. Anselma and G. Belingardi are with the Department of Mechanical and Aerospace Engineering (DIMEAS), Politecnico di Torino, Torino 10129, Italy (e-mail: pier.anselma@polito.it; giovanni.belingardi@polito.it).

Y. Huo, J. Roeleveld and A. Emadi are with the McMaster Institute for Automotive Research and Technology (MacAUTO), McMaster University, Hamilton ON L8P0A6, Canada (email: huoy@mcmaster.ca; roelej@mcmaster.ca; emadi@mcmaster.ca).

hybrid electric vehicle transmission [27].

Nevertheless, all the strategies illustrated above present some drawbacks: the ECMS does not guarantee the global optimum and requires the calibration of the tuning factor for the electrical energy consumption. DP can achieve the globally optimal solution; but, it suffers from consistent computational burden necessary for the exhaustive search followed by an iterative calculation. The PEARS algorithm is computationally rapid and it can satisfy the charge-sustaining criterion without recurring to iterative calculation, however it exhibits non-uniform proximity with the global optimum. Therefore, there still remains a need for a validated off-line control strategy suitable for rapid sizing of multimode HEVs.

This paper consequently introduces a novel approach to the off-line energy management problem for HEVs that aims at exploiting the advantages and minimizing the drawbacks of each aforementioned optimization method. Particularly, the slope-weighted energy-based rapid control analysis (SERCA) for HEVs is based on first-order derivatives and energy balance. Improving the performance of HEV control and ameliorating the effectiveness of HEV powertrain design methodologies through consistent reduction of computational effort are the main targets of the introduction of SERCA. These objectives are demonstrated by SERCA exhibiting the best trade-off between fuel economy optimality and computational burden compared to the other control strategies.

Organization of the paper is as follows: the HEV configuration under study is presented and modeled. The novel energy management strategy is then illustrated and detailed. Subsequently, simulation results in MATLAB© software for different control strategies are compared highlighting the performance of SERCA. Conclusions are finally given.

II. Vehicle and Powertrain Model

The HEV power-split powertrain retained in this paper comes from the industrial state-of-art and integrates two electric motor/generators (MGs) and an ICE [28]. The correspondent double PG lever diagram, accompanied by its gear parameters, is shown in Fig. 1. The HEV can operate in electric or hybrid mode according to the grounding clutch being engaged or disengaged.

In general, a vehicle model constituted by analytical equations is simulated in a backward quasi-static approach [29]. Detailed modeling for the components of the considered HEV powertrain is presented as follows.

A. Road load and vehicle

The requested torque at the output shaft of the PG2 can be evaluated at each time step using (1).

$$T_{out} = \left(F_{road} + I_v \cdot \frac{a}{{r_{dyn}}^2}\right) \cdot \frac{r_{dyn}}{\tau} \quad (1)$$

F_{road} represents the road resistance forces (evaluated using experimental road load coefficients [27]), I_v is the vehicle equivalent inertia evaluated at the wheel shaft, a represents the vehicle acceleration calculated from the vehicle speed in adjacent time points. r_{dyn} and τ are the wheel rolling radius and the final drive ratio, respectively.

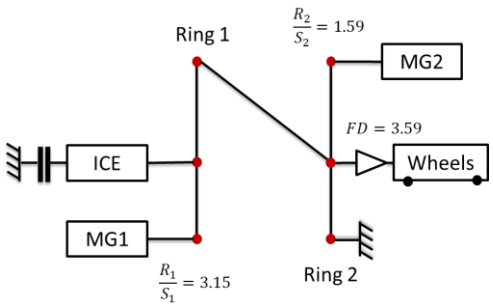

Fig. 1. Lever diagram of the HEV powertrain under study

B. Hybrid transaxle

Looking at Fig. 1, the MG2 operating speed ω_{MG2} is proportionally constrained to the output speed ω_{out}, while the MG1 speed ω_{MG1} is a function of the ICE speed ω_{ICE} (which is a defined control variable). The kinematic constraints can thus be summarized in (2).

$$\begin{bmatrix}\omega_{MG1}\\ \omega_{MG2}\end{bmatrix} = \begin{bmatrix}-R_1/S_1 & \frac{R_1}{S_1}+1\\ \frac{R_2}{S_2}+1 & 0\end{bmatrix}\begin{bmatrix}\omega_{out}\\ \omega_{ICE}\end{bmatrix} \quad (2)$$

R and S represent the number of teeth for the ring and the sun of the PGs, respectively. When the ICE is grounded through the clutch in electric operation, ω_{ICE} is set to 0. Assuming unitary efficiency for the transmission, the torque split between the two PGs can be determined arbitrarily to satisfy the output energy demand.

C. Power components

Once the torque and speed values are determined for the MGs, the requested battery output power P_{batt} can be evaluated using (3).

$$P_{batt} = \sum_{k=1}^{2} \omega_{MGk} \cdot T_{MGk} \cdot \eta_{MGk}^{-sign(T_{MGk})} \quad (3)$$

η_{MG} are the efficiency values of the MGs, evaluable by numerical efficiency maps including inverter efficiencies. The rate of battery State-of-Charge (SOC), $\dot{SOC}$, can thus be calculated in (4) adopting an equivalent open circuit model.

$$\dot{SOC} = \frac{\sqrt{{V_{OC}}^2 - 4 \cdot R_{IN} \cdot P_{batt}} - V_{OC}}{2 \cdot R_{IN} \cdot Q_{batt}} \quad (4)$$

V_{OC}, R_{IN} and Q_{batt} are the output voltage, the internal resistance and the capacity of the battery, respectively. Particularly, R_{IN} and V_{OC} are assumed to be independent from the SOC since a previous study demonstrated that it is still possible to achieve a globally optimal solution with this hypothesis [30].

The fuel consumption can be evaluated as well from an experimental furl flow map of the considered ICE with torque and speed as independent variables.

III. Optimal Control of HEVs

The optimal control problem for an HEV aims at minimizing the estimated fuel consumption (EFC) over a certain period. The resulting mathematical formulation is stated in (5):

$$\min\left\{ J = \int_{t_0}^{t_{end}} L(\omega_{ICE}, T_{ICE}, t)dt \right\}$$

subject to:

$$\begin{aligned} & SOC(t_0) = SOC(t_{end}) \\ & \dot{SOC} = f(SOC, \omega_{MG1}, T_{MG1}, \omega_{MG2}, T_{MG2}) \\ & \omega_{ICE\,min} \le \omega_{ICE} \le \omega_{ICE\,MAX} \\ & \omega_{MG1\,min} \le \omega_{MG1} \le \omega_{MG1\,MAX} \\ & \omega_{MG2\,min} \le \omega_{MG2} \le \omega_{MG2\,MAX} \\ & T_{ICE\,min} \le T_{ICE} \le T_{ICE\,MAX} \\ & T_{MG1\,min} \le T_{MG1} \le T_{MG1\,MAX} \\ & T_{MG2\,min} \le T_{MG2} \le T_{MG2\,MAX} \\ & P_{batt\,min} \le P_{batt} \le P_{batt\,MAX} \end{aligned} \quad (5)$$

Where $L(\omega_{ICE}, T_{ICE}, t)$ represents the instantaneous rate of fuel consumption. Charge-sustaining (CS) criteria is defined by imposing equivalent battery SOC values at the beginning and the end of the considered time period. Finally, speed and torque of power components are restricted within the correspondent actual operating regions. The most common approaches to solve the illustrated problem can be briefly described as below.

A. Equivalent Consumption Minimization Strategy

The ECMS represents a direct derivation of the PMP, which consists of a general case of the Euler-Lagrange equation in the calculus of variation. The key idea of ECMS is that, in both charge and discharge, an equivalent fuel consumption can be associated with the use of electrical energy. The total instantaneous equivalent fuel consumption $\dot{m}_{fuel_{eq}}$ can thus be defined in (6):

$$\dot{m}_{fuel_{eq}} = \dot{m}_{fuel\_ICE} + \dot{m}_{fuel\_elec} \quad (6)$$

Where $\dot{m}_{fuel\_elec}$ represents the equivalent fuel consumption of the HEV electrical power path and can be calculated in (7).

$$\dot{m}_{fuel\_elec} = \frac{s(t)}{Q_{LHV}} P_{batt}(t) \quad (7)$$

Q_{LHV} is the fuel lower heating value, while $s(t)$ represents a constant equivalence factor which assigns a cost to the use of electricity, thus converting electrical power from the battery into equivalent fuel consumption. $s(t)$ can be tuned by minimizing the Hamiltonian derived from ICE fuel consumption and battery SOC variation, as stated in [31].

Using a single equivalence factor allows estimating the fuel consumption regardless of the torque and speed of power components. However, accuracy may be questionable when the operating conditions change. Moreover, tuning the equivalence factor may result computationally inefficient when dealing with component sizing in the HEV powertrain design procedure.

B. Dynamic Programing

DP is by far the most commonly adopted approach to solve the HEV optimal control problem. It involves generating a globally optimal solution backward along a time horizon by searching through all feasible discrete control actions for all the state grid points [32]. This translates for the HEV powertrain control problem in the minimization of the cost function illustrated in (8) over the considered time horizon [23].

$$J = \sum_{k=0}^{N-1} \left(\dot{m}_{fuel_k} + \alpha \cdot \Delta SOC^2 \right)$$

$$\Delta SOC = \begin{cases} SOC_k - SOC_{target} & SOC_k < SOC_{target} \\ 0 & SOC_k \ge SOC_{target} \end{cases} \quad (8)$$

SOC_{target} is the desired value of battery SOC, while α represents an operating factor. While DP is demonstrated achieving global optimality under a wide range of operating conditions, its major drawback refers to the computational power needed for exhaustively searching through all the possible solutions [33].

C. Power-weighted Efficiency Analysis for Rapid Sizing

The Power-weighted Efficiency Analysis for Rapid Sizing (PEARS) has been introduced by Zhang et al. as a near-optimal control strategy for HEVs [24]. In the PEARS algorithm, overall efficiency values for each mode are retained as the weighting factor for selecting hybrid or electric powertrain operation. Beforehand, speed and torque of power components are swept to determine the optimal combination in terms of mode efficiency at each driving cycle point.

Once the entire driving cycle is analyzed to extract the efficiency-based optimal power split for each operating mode at each time step, the powertrain is initially set to operate in electric modes only (the most efficient mode to achieve the speed and torque output). Subsequently, a recursive process starts that aims at replacing electric with hybrid operation in the driving cycle points where the smallest ranges between hybrid and electric mode efficiencies are observed. This iterative procedure is conducted until the charge-balance is realized and the battery State-of-Charge (SOC) exhibits equal values at the beginning and at the end of the driving cycle. The mode-shifting schedule and the resulting fuel consumption can be evaluated in this way. Details regarding the operation of the algorithm can be found in [26].

IV. The Slope-weighted Energy-based Rapid Control Analysis

In this section, the Slope-weighted Energy-based Rapid Control Analysis (SERCA) is introduced as a novel approach for the HEV optimal control problem. This methodology can be divided in three phases, as illustrated in Fig. 2: the division into sub-problems, the definition of the generalized optimal operating points and the energy balance realization process.

A. Sub-problems Exploration

The first step of SERCA aims at exploring the possible solutions of each sub-problem, particularly represented by the single drive cycle point. The sub-problems are characterized with the specific values of current vehicle speed and desired acceleration, respectively. The exploration of the possible solutions can be performed in three stages: the discretization of the control variables, the solutions formation via operating constraints consideration and the solutions evaluation. A graphical interpretation of these stages can be observed in Fig. 3.

This article has been accepted for publication in a future issue of this journal, but has not been fully edited. Content may change prior to final publication. Citation information: DOI 10.1109/TVT.2019.2899360, IEEE Transactions on Vehicular Technology

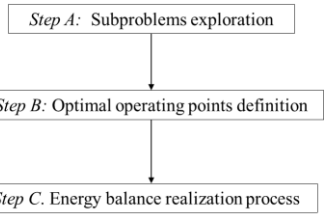

Fig. 2. Workflow of SERCA

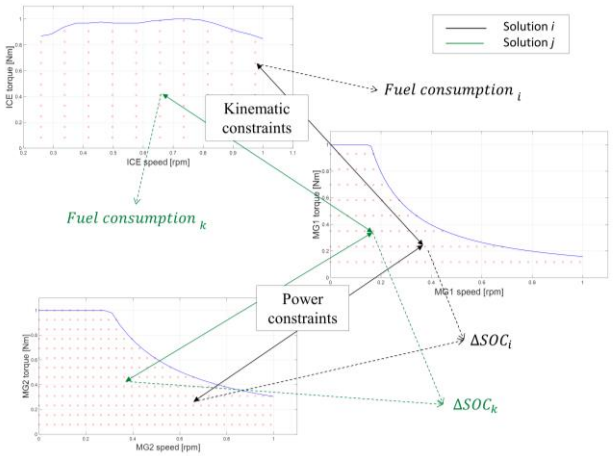

Fig. 3. Discretization, relationships and outcomes related to the control variables

1) Discretization of the control variables

The torque and speed maps of the power components can be discretized based on selected resolution values, as performed in the traditional DP technique. The red operating points of Fig. 3 are thus obtained, respecting the limits imposed by the maximum torque curves.

2) Solutions formation

The solutions for a sub-problem are constituted by specific combinations of operating points for the power components. These can be found by appropriately sweeping the operating points from the power component maps previously identified. Each solution is required to satisfy two performance requirements:

- the PG kinematic constraints imposed in (2)
- the algebraic sum of the mechanical powers provided by the components must equal the requested output power.

As example, Fig. 3 reports two possible solutions where the two-way arrows may represent operating constraints for the solutions. Both hybrid and pure electric operations are considered in this process.

3) Solutions evaluation

After all the possible solutions for the sub-problem are identified, their performance can be evaluated. Particularly, the correspondent fuel consumption can be assessed through the fuel map, while the variation in the battery SOC can be calculated using (3) and (4). The dashed arrows in Fig. 3 represent a graphical interpretation of this step.

B. Generalized Optimal Operating Points Definition

Once all the possible solutions are identified for a specific sub-problem(i.e. a target cycle point), they can be assessed based on fuel consumption and battery SOC variation, as illustrated in Fig. 4. The general descending trend of the point cloud reminds how battery recharging can be achieved through the gradual increase of fuel consumption. This representation can be interpreted as a sort of Pareto frontier for all the operating solutions of the HEV powertrain in the considered sub-problem. The solutions at the lower edge of the point cloud thus correspond to the optimal ones, as they exhibit the highest ratio between charged battery energy and correspondently consumed fuel. As consequence, these points should be considered for eventual hybrid operation in an attempt of reaching the global optimal solution in a considered drive cycle. In the ECMS a similar approach is employed to derive an optimal engine operating line [30], however the SERCA considers discrete operating points rather than continuous variables.

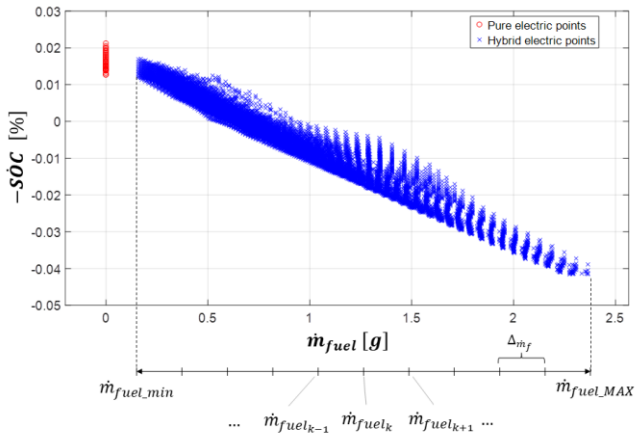

Fig. 4. Example of solutions comparison for a sub-problem

The next step aims at identifying the optimal solutions for the considered sub-problems and storing them in a variable used in the following stage to solve the overall drive cycle control problem. This procedure can be divided in different sub-steps:

1) Discretization of the fuel consumption interval

The fuel consumption interval for the considered sub-problem is represented by the span $[\dot{m}_{fuel\_min}, \dot{m}_{fuel\_MAX}]$ of Fig. 4. This interval is discretized with a selected number of equidistant points $\dot{m}_{fuel_k}$. The number of points is set to 15 in this paper as a result of the sensitivity study conducted later in this section.

2) Optimal solutions identification

A correspondent optimal solution can be identified for each selected point of the fuel consumption interval. Referring to Fig. 4, the formulation of this problem related to the general point $\dot{m}_{fuel_k}$ can be expressed in (9).

$$\min[\dot{SOC}(\dot{m}_{fuel})]$$
$$\text{subject to: } \dot{m}_{fuel} \in \left[\left(\dot{m}_{fuel_k} - \frac{\Delta_{\dot{m}_f}}{2}\right); \left(\dot{m}_{fuel_k} + \frac{\Delta_{\dot{m}_f}}{2}\right)\right] \quad (9)$$

Repeating this operation for each member of the discretized fuel consumption interval thus returns a vector representing the discrete hull of the optimal solutions for the considered sub-problem.

This article has been accepted for publication in a future issue of this journal, but has not been fully edited. Content may change prior to final publication. Citation information: DOI 10.1109/TVT.2019.2899360, IEEE Transactions on Vehicular Technology

TABLE I
STORED VARIABLE FOR THE TARGET CYCLE

Target cycle point	Optimal hybrid point #1	…	Optimal hybrid point *k*	…	Optimal hybrid point #20
…	…	…	…	…	…
i-1	$p_{i-1,1}$, $u_{i-1,1}$	…	$p_{i-1,k}$, $u_{i-1,k}$	…	$p_{i-1,20}$, $u_{i-1,20}$
i	$p_{i,1}$, $u_{i,1}$	…	$p_{i,k}$, $u_{i,k}$	…	$p_{i,20}$, $u_{i,20}$
i+1	$p_{i+1,1}$, $u_{i+1,1}$	…	$p_{i+1,k}$, $u_{i+1,k}$	…	$p_{i+1,20}$, $u_{i+1,20}$
…	..	…	…	…	…

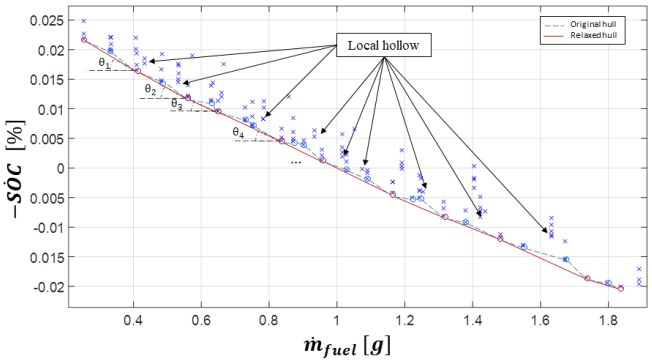

Fig. 5. Example of discrete optimal hull identification for a sub-problem

3) Slope-based relaxation

The discrete hull identified above generally presents considerable irregularities, as illustrated in Fig. 5. Particularly local hollows, characterized by a lack of increase in the battery SOC despite increasing the fuel consumption, can be frequently observed. These local concave regions may prevent the optimization algorithm from descending along the optimal hull, thus reducing the probability to achieve an optimal solution. As consequence, a filtration technique should be applied to overcome this draft. In this procedure the points of the discrete hull are evaluated backward starting from $\dot{m}_{fuel\_MAX}$ to $\dot{m}_{fuel\_min}$. The generic point *k* is then maintained if the condition expressed in (10) is respected, otherwise it is discarded from the variable memorizing the hull.

$$\dot{SOC}\left(\dot{m}_{fuel_k}\right) < \dot{SOC}\left(\dot{m}_{fuel_{k+1}}\right) \tag{10}$$

The discretized light blue hull of Fig. 5 is obtained in this way. This nevertheless exhibits a persistently fluctuating trend, which may subsequently cause the same issues described above for the local hollows. As consequence, a relaxation of the hull should be performed in order to enhance its convexity. The slope between two adjacent points of the optimal hull is firstly defined as θ in (11).

$$\theta(k-1,k) = \frac{\Delta \dot{SOC}}{\Delta \dot{m}_{fuel}} = \frac{\dot{SOC}(k) - \dot{SOC}(k-1)}{\dot{m}_{fuel}(k) - \dot{m}_{fuel}(k-1)} \tag{11}$$

The relaxation technique applied in this paper consists in examining the points of the hull backward once more verifying the discrimination criteria for adjacent points presented in (12).

$$|\theta(k-1,k)| \geq |\theta(k,k+1)| \tag{12}$$

The point *k* is maintained or discarded according to condition (8) being respected or not. This allows obtaining the relaxed hull displayed in red in Fig. 5. Smooth trend with steeper slopes at lower levels of fuel consumption can be obtained in this way. Each point of the discretized hull in the stored variable is accompanied with the correspondent slope value θ, as illustrated in Fig. 5.

TABLE II
VEHICLE AND POWERTRAIN DATA

Component	Parameter	Value
Vehicle	Mass	2248 Kg
	Wheel dynamic radius	0.358 m
ICE	Capacity	3.3 L
	Maximum power	188 kW @ 5800 rpm
	Maximum torque	320 Nm @ 4400 rpm
MG1	Maximum power	60 kW
MG2	Maximum power	85 kW
Battery	V_{OC}	359 V
	$R_{IN\_charging}$	0.0898 Ω
	$R_{IN\_discharging}$	0.0984 Ω
	Q_{batt}	18.5 kWh

Once the steps described above are repeated for each sub-problem, i.e. all the time points of the target cycle, the results can be stored in a variable presenting the structure illustrated in TABLE I. *p* represents the control variables related to the operating point (i.e. torque and speed of power components), while *u* contains the correspondent state variables and can be described in (13) for the generic point *k* of the discretized convex hull for the target cycle point *i*.

$$\begin{aligned} u_{1|_{i,k}} &= \theta_i(k-1,k) \\ u_{2|_{i,k}} &= \dot{SOC}_i(k) - \dot{SOC}_i(k-1) \\ u_{3|_{i,k}} &= \dot{m}_{fuel_i}(k) - \dot{m}_{fuel_i}(k-1) \end{aligned} \tag{13}$$

An additional variable is created containing the state and control variables related to the optimal pure electric solution for each point of the target cycle. Hence, the state variables $\{u\}$ for the first column in TABLE I take into account the pure electric solutions for the values related to the column (*k-1*).

C. Energy Balance Realization

The last step of the SERCA technique aims at efficiently solving the optimal control problem for the overall considered target cycle. This procedure has been inspired by the energy-balance realization method adopted in the PEARS algorithm [26]. The flowchart of this step is illustrated in Fig. 6 and detailed as follows:

1) Step C.1: First it is assumed that, when possible, all the target cycle points operate in the pure electric mode. Particularly, in the Pareto frontier of Fig. 3 the pure electric point with the lowest $\dot{SOC}$ is retained and the powertrain is set to operate according to the correspondent control variables in the considered target cycle point. The total required electrical energy E_{EV} is subsequently obtained by the sum of the battery energy consumption in each point where pure electric mode is operable. The global fuel consumption m_{fuel_TOT} is set to 0.

2) Step C.2: From the first column of the variable illustrated in TABLE I, the target cycle point *i* exhibiting the highest value of slope ($|\theta_i| = |\theta_{MAX}|$) is retained for hybrid operation. The correspondent control variables are set to operate in the target cycle point.

This article has been accepted for publication in a future issue of this journal, but has not been fully edited. Content may change prior to final publication. Citation information: DOI 10.1109/TVT.2019.2899360, IEEE Transactions on Vehicular Technology

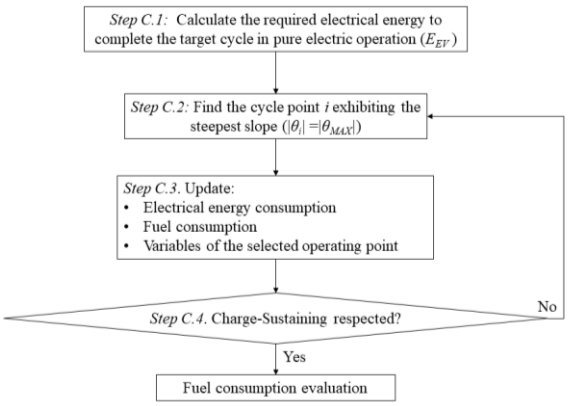

Fig. 6. Flowchart of step C

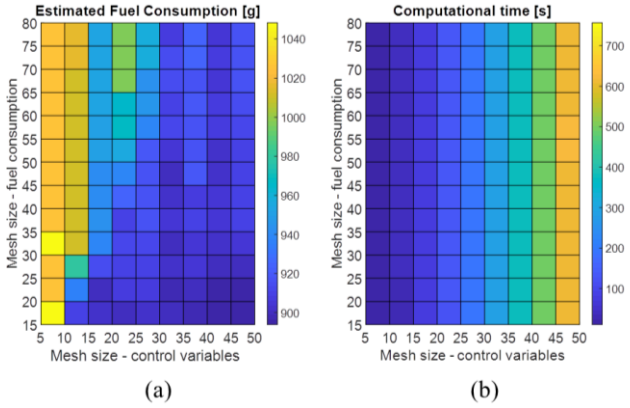

Fig. 7. Sensitivity study of SERCA parameters

3) Step C.3: Once the target cycle point *i* is selected, the variables related to the overall target cycle operation are updated in (14). Particularly, the value of electrical energy needed is reduced by the control variable (negative) value corresponding to the selected point *i*. Meanwhile, the global fuel consumption m_{fuel_TOT} is increased with the increment provided by the selected hybrid operating point.

$$\begin{aligned} \mathrm{E}_{EV} &= \mathrm{E}_{EV} + u_{2|_{i,1}} \\ \mathrm{m}_{fuel\_TOT} &= \mathrm{m}_{fuel\_TOT} + u_{3|_{i,1}} \end{aligned} \tag{14}$$

Finally, the state and control variables for point *i* need to be updated in (15) after being selected. In other words, a left shift is performed in row i^{th} of the variable of TABLE I (e.g. values of cell (*i,2*) become the values of cell (*i,1*)). This operation allows considering the adjacent hull point for the target cycle point *i* in the following iteration of the algorithm.

$$\begin{aligned} \left\{u_{|i,k}\right\} &= \left\{u_{|i,k+1}\right\} \\ \left\{p_{|i,k}\right\} &= \left\{p_{|i,k+1}\right\} \end{aligned} \tag{15}$$

4) Step C.4: A check is conducted for the CS operation being respected. This corresponds to the value of E_{EV} being null or negative. If this condition is not respected, steps C.2 and C.3 are iterated. Otherwise, the algorithm is concluded and the correspondent fuel consumption, together with the overall powertrain operation for the target cycle, can be extrapolated.

A sensitivity study is performed here to assess the discretization of both the control variables and the fuel consumption interval. TABLE II illustrates the vehicle and powertrain data considered in this paper. Particularly, several simulations are run considering the HEV controlled off-line by SERCA in the worldwide harmonized light vehicle test procedure (WLTP) cycle. Fig. 7 reports the obtained results, where the two axis refer to the number of equidistant points retained to discretized the fuel consumption intervals and the control variables, respectively. Fig. 7 (a) demonstrates how consistent fuel economy results can be achieved even with small mesh sizes. As regards the control variables, a consistent reduction of the predicted fuel consumption is observed between the mesh sizes of 5 and 15, followed by a quite constant trend. On the other hand, increasing the mesh size for the fuel consumption interval (i.e. more than 30 points) may lead the algorithm to operate ineffectively, especially at small control variable discretization intervals. The required computational time (CT) in Fig. 7 increases proportionally to the mesh size for the control variables, while it is overall constant with respect to the increase of discretization points for the fuel consumption interval. As a results, the value of 15 for both the discretization processes may be adopted to combine optimality of fuel economy and computational advantage.

V. Simulation Results

The SERCA technique aims at combining global optimality for the HEV control problem solution and simultaneous light-weighting of the computational burden. In this section, two different analysis validate the proposed control strategy for HEVs powertrain. In the first one, a comprehensive sensitivity study is performed assessing the EFC and the correspondently required CT for SERCA, PEARS and DP. Then, four different drive cycles are considered to evaluate the performance of the aforementioned strategies together with ECMS. ECMS, DP and PEARS are particularly retained as benchmark energy management strategies for the SERCA algorithm. All the reported CTs refer to a desktop computer with Intel Core i7-8700 (3.2 GHz) and 32 GB of RAM. In all the simulations, a CS operation has been simulated by imposing equal battery SoC values at the beginning and the end of the drive cycles.

This article has been accepted for publication in a future issue of this journal, but has not been fully edited. Content may change prior to final publication. Citation information: DOI 10.1109/TVT.2019.2899360, IEEE Transactions on Vehicular Technology

A. *Sensitivity Study*

PEARS, SERCA and DP are specially selected for the sensitivity study as they are commonly employed in design and sizing techniques for power–split HEVs. ECMS would indeed require recursive tuning of the equivalence factor, thus resulting unpractical [34].

In this study, control variables are discretized according to an equal number of equidistant points, referred to the mesh size. 15 points are retained for discretizing the fuel consumption interval of SERCA, as demonstrated in the previous section. Therefore, the sensitivity of both SERCA and PEARS algorithms only depends on the mesh size of the control variables. On the other hand, the operation of DP is affected by the discretization of the state grid (i.e. the battery SoC) [33]. Four different values of mesh size are consequently retained for the state grid of DP: 20, 50, 100 and 500. The sensitivity study is conducted simulating the retained HEV controlled off-line in the WLTP by the considered algorithms and varying the mesh size for the control variables and the state grid. Obtained results are illustrated in Fig. 8. Concerning DP, only values up to 45 were considered for the control variables mesh size related to the case of 500 SoC points. Indeed, increasing the mesh size would have led to excessively long CTs. As expected, increasing the mesh size reduces the EFC. However, this improvement drastically reduces after a certain value of mesh size for all the three algorithms. The SERCA algorithm is found remarkably improving the EFC compared to PEARS, while maintaining consistent CT. On the other hand, EFC values for PEARS and DP are similar only for reduced state grid mesh sizes (i.e. 20 and 50). On its behalf, the SERCA algorithm demonstrates obtaining EFC results comparable with DP even with increased state grid mesh sizes (i.e. 100 and 500), while reducing the corresponding CT by near two orders of magnitude.

B. *Benchmark Study*

In this paragraph, the operation of SERCA, PEARS, DP and ECMS are assessed for different drive cycles. These particularly include the Urban Dynamometer Driving Schedule (UDDS), the Highway Federal Test Procedure (HWFET), the New European Driving Cycle (NEDC) and the WLTP. The mesh size for the control variables has been selected based on the lowest value for which the EFC of DP overtakes the one of SERCA in Fig. 8, thus 30. The mesh size for the state grids of DP has been set to 100 to reduce the corresponding CT. As regards the ECMS, the equivalence factor $s(t)$ has been tuned for each drive cycle according to the CS criterion. TABLE III and TABLE IV report the obtained results for EFC and CT, respectively. The EFC values in TABLE III are in line with the global optimality principle of DP, with the remaining considered strategies achieving near-optimal results. For this particular HEV powertrain, the PEARS algorithm is revealed to under-perform with respect to the other strategies, exhibiting as instance an EFC increase of near 69% for the WLTP case with respect to DP. On the other hand, in TABLE IV PEARS establishes itself as the most rapid control strategy, while DP requires a CT greater by near two orders of magnitude. ECMS achieves appreciable results both in terms of EFC and CT,

TABLE III
SIMULATION RESULTS – EFC

	SERCA	PEARS	DP	ECMS
WLTP	896.7 g (+0.5 %)	1108.0 g (+24.1 %)	892.6 g	944.9 g (+5.9 %)
UDDS	275.6 g (+0.8 %)	443.3 g (+62.1 %)	273.4 g	305.7 g (+10.8 %)
HWFET	633.9 g (+0.4 %)	747.9 g (+18.5 %)	631.3 g	697.6 g (+10.5 %)
NEDC	341.3 g (+0.3 %)	574.2 g (+68.7 %)	340.4 g	362.0 g (+6.4 %)

TABLE IV
SIMULATION RESULTS – CT

	SERCA	PEARS	DP	ECMS
WLTP	283 s	250 s	357.2 min	302 s
UDDS	193 s	158 s	154.7 min	211 s
HWFET	171 s	148 s	105.5 min	188 s
NEDC	158 s	133 s	131.9 min	175 s

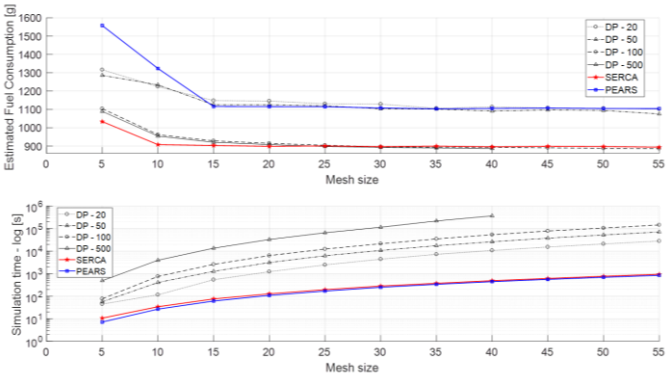

Fig. 8 Comparison of SERCA, PEARS and DP

however this comparison does not account for the needed calibration of the equivalence factor. On its behalf, SERCA demonstrates both consistent proximity with the globally optimal EFC solution and rapidness close to the PEARS algorithm.

Explanation for the PEARS ineffectiveness for this dual-mode HEV powertrain can be related to the consideration of the overall powertrain efficiency value only when optimizing the entire target cycle operation. This translates in a single optimized point retained for each mode at each target cycle point, thus limiting the overall operational flexibility. However, when multiple modes are available, the EFC numerical distance between PEARS and the globally optimal solution can be significantly reduced. This correlates with the PEARS algorithm originally designed for rapid sizing of multimode HEV powertrains, where it is proved to achieve results similar to DP [24][34]. In this framework, the SERCA reveals more efficient compared to the current state-of-art, particularly when considering HEV powertrains with few operating modes. At the same time, the objective realization of the charge-sustaining operation allows avoiding recursive calculation thus enabling the implementation of SERCA for effective rapid sizing of powertrain components.

VI. CONCLUSIONS

This paper introduces a novel rapid near-optimal energy management strategy for HEV powertrains named slope-weighted energy-based rapid control analysis (SERCA). The operating steps of the SERCA techniques have been detailed, particularly the division into sub-problems, the construction of the generalized optimal operating hulls and the energy balance realization process.

The SERCA addresses the problem of effective rapid component sizing for HEV powertrains with different grades of multimodality. This novel technique has been elaborated based on optimization concepts coming from different HEV energy management strategies. The division into sub-problems and their efficient exploration have been inherited from DP; the generation of the discrete optimal operating hull is derived from the instantaneous optimization of the Hamiltonian in the ECMS, while the objective realization of the charge-balanced operation comes from the PEARS algorithm procedure.

The illustrated energy management strategy is validated based on two different analysis. First, an exhaustive sensitivity study is conducted to assess the behavior of SERCA, DP and PEARS according to the selected operating parameters. Then, SERCA, DP, PEARS and ECMS control strategies are simulated considering different drive cycles. The comparison of the resulting SERCA EFC with the globally optimal solution provided by DP reveals a narrow difference contained within 1%. Moreover, the SERCA technique is demonstrated achieving computational rapidness similar to the PEARS algorithm, while remarkably improving its EFC. Future work may consider the implementation of the SERCA in a design methodology for rapid component sizing of multimode power split HEV powertrains. Particularly, differences in the identified resulting optimal design may be expected compared to the current design methodologies that employ the PEARS algorithm [24][27]. Finally, an on-line energy management strategy may be developed based on the SERCA and implemented in an on-board control logic. For instance, off-line SERCA optimization may be considered to derive optimal control policies [35]. Alternatively, the rapidness of SERCA may be associated to recent advances in intelligent transportation systems to establish on-line optimal adaptive HEV control strategies [36].

REFERENCES

[1] B. Bilgin et al., "Making the Case for Electrified Transportation," in *IEEE Transactions on Transportation Electrification*, vol. 1, no. 1, pp. 4-17, 2015.

[2] N.E. Boudette, "European Automakers Prepare for an Electric Future," in *New York Times*, 6 March 2018.

[3] A. Emadi, "Transportation 2.0: Electrified-Enabling cleaner, greener, and more affordable domestic electricity to replace petroleum," in *IEEE Power Energy Mag.*, vol. 9, no. 4, pp. 18–29, 2011.

[4] S. S. Williamson and A. Emadi, "Comparative assessment of hybrid electric and fuel cell vehicles based on comprehensive well-to-wheels efficiency analysis," in *IEEE Transactions on Vehicular Technology*, vol. 54, no. 3, pp. 856-862, 2005.

[5] A. Emadi, K. Rajashekara, S. Williamson, S. Lukic, "Topological Overview of Hybrid Electric and Fuel Cell Vehicular Power System Architectures and Configurations," in *IEEE Transactions on Vehicular Technology*, vol. 54, no. 3, pp. 763-770, 2005.

[6] 5. S. M. Lukic and A. Emadi, "Effects of drivetrain hybridization on fuel economy and dynamic performances of parallel hybrid electric vehicles," in *IEEE Transactions on Vehicular Technology*, vol. 53, pp. 385–389, 2004.

[7] Y. Yang, K. Arshad-Ali, J. Roeleveld, A. Emadi, "State-of-the-art electrified powertrains – hybrid, plug-in, and electric vehicles", in *Int. J. Powertrains*, 2016; 5,(1), pp. 1-29.

[8] X. Zhang, C. T. Li, D. Kum and H. Peng, "Prius+ and Volt-: Configuration Analysis of Power-Split Hybrid Vehicles With a Single Planetary Gear," in *IEEE Transactions on Vehicular Technology*, vol. 61, no. 8, pp. 3544-3552, 2012.

[9] B. Mashadi and S. A. M. Emadi, "Dual-Mode Power-Split Transmission for Hybrid Electric Vehicles," in *IEEE Transactions on Vehicular Technology*, vol. 59, no. 7, pp. 3223-3232, 2010.

[10] Y. Yang, N. Schofield and A. Emadi, "Integrated Electromechanical Double-Rotor Compound Hybrid Transmissions for Hybrid Electric Vehicles," in *IEEE Transactions on Vehicular Technology*, vol. 65, no. 6, pp. 4687-4699, 2016.

[11] I. J. Albert, E. Kahrimanovic, and A. Emadi, "Diesel Sport Utility Vehicles With Hybrid Electric Drive Trains," in *IEEE Transactions on Vehicular Technology*, vol. 53, No. 4 pp. 1247–1256, 2004.

[12] S. S. Williamson, S. G. Wirasingha, and A. Emadi, "Comparative Investigation of Series and Parallel Hybrid Electric Drive Trains for Heavy-Duty Transit Bus Applications," in *Conf. IEEE-VPPC*, 2006, pp. l-l0.

[13] A. Somà, F. Bruzzese, F. Mocera and E. Viglietti, "Hybridization Factor and Performance of Hybrid Electric Telehandler Vehicle," in *IEEE Transactions on Industry Applications*, vol. 52, no. 6, pp. 5130-5138, 2016.

[14] S. G. Li, S. M. Sharkh, F. C. Walsh and C. N. Zhang, "Energy and Battery Management of a Plug-In Series Hybrid Electric Vehicle Using Fuzzy Logic," in *IEEE Transactions on Vehicular Technology*, vol. 60, no. 8, pp. 3571-3585, Oct. 2011.

[15] S. G. Wirasingha and A. Emadi, "Classification and Review of Control Strategies for Plug-In Hybrid Electric Vehicles," in *IEEE Transactions on Vehicular Technology*, vol. 60, no. 1, pp. 111-122, Jan. 2011.

[16] Paganelli, G., Guezennec, Y., and Rizzoni, G., "Optimizing Control Strategy for Hybrid Fuel Cell Vehicle," *SAE Technical Paper* 2002-01-0102, 2002.

[17] S. Delprat, T. Hofman and S. Paganelli, "Hybrid Vehicle Energy Management: Singular Optimal Control," in *IEEE Transactions on Vehicular Technology*, vol. 66, no. 11, pp. 9654-9666, Nov. 2017.

[18] R. E. Bellman, *Dynamic Programming*, Princeton, NJ: Princeton Univ. Press, 1957.

[19] Auiler, J.E., Zbrozek, J.D., Blumberg, P.N., "Optimization of automotive engine calibration for better fuel economy- methods and applications", in *SAE International Automotive Engineering Congress and Exposition*, 1977.

[20] S. Delprat, J. Lauber, T. M. Guerra, and J. Rimaux," Control of a Parallel Hybrid Powertrain: Optimal Control," in *IEEE Transactions on Vehicular Technology*, vol. 53, no. 3, may 2004.

[21] Q. Gong, Y. Li and Z. R. Peng, "Trip-Based Optimal Power Management of Plug-in Hybrid Electric Vehicles," in *IEEE Transactions on Vehicular Technology*, vol. 57, no. 6, pp. 3393-3401, Nov. 2008.

[22] R. Wang and S. M. Lukic, "Dynamic programming technique in hybrid electric vehicle optimization," *2012 IEEE International Electric Vehicle Conference*, Greenville, SC, 2012, pp. 1-8.

[23] J. Liu and H. Peng, "Modeling and Control of a Power-Split Hybrid Vehicle," in *IEEE Transactions on Control Systems Technology*, vol. 16, no. 6, pp. 1242-1251, Nov. 2008.

[24] X. Zhang, H. Peng, J. Sun, "A near-optimal power management strategy for rapid component sizing of power split hybrid vehicles with multiple operating modes," in *American Control Conference(ACC)*, 2013, pp.5972-5977.

[25] X. Zhang, S. E. Li, H. Peng and J. Sun, "Design of Multimode Power-Split Hybrid Vehicles—A Case Study on the Voltec Powertrain System," in *IEEE Transactions on Vehicular Technology*, vol. 65, no. 6, pp. 4790-4801, June 2016.

[26] P.G. Anselma, Y. Huo, E. Amin, J. Roeleveld, A. Emadi, G. Belingardi, "Mode-shifting Minimization in a Power Management Strategy for Rapid Component Sizing of Multimode Power Split Hybrid Vehicles," *SAE Technical Paper* 2018-01-1018, 2018.

[27] P.G. Anselma, Y. Huo, J. Roeleveld, A. Emadi, G. Belingardi, "Rapid optimal design of a multimode power split hybrid electric vehicle transmission", *Proc. IMechE Part D: J. Automobile Engineering*, online Jan. 2018.

[28] Pittel, M. and Martin, D., "eFlite Dedicated Hybrid Transmission for Chrysler Pacifica," *SAE Technical Paper* 2018-01-0396, 2018.
[29] L. Guzzella and A. Amstutz, "CAE tools for quasi-static modeling and optimization of hybrid powertrains," in *IEEE Transactions on Vehicular Technology*, vol. 48, no. 6, pp. 1762-1769, Nov 1999.
[30] N. Kim, S. Cha and H. Peng, "Optimal Control of Hybrid Electric Vehicles Based on Pontryagin's Minimum Principle," in *IEEE Transactions on Control Systems Technology*, vol. 19, no. 5, pp. 1279-1287, Sept. 2011.
[31] N. Kim, S. W. Cha and H. Peng, "Optimal Equivalent Fuel Consumption for Hybrid Electric Vehicles," in *IEEE Transactions on Control Systems Technology*, vol. 20, no. 3, pp. 817-825, May 2012.
[32] O. Sundstrom and L. Guzzella, "A generic dynamic programming Matlab function," *2009 IEEE Control Applications, (CCA) & Intelligent Control, (ISIC)*, St. Petersburg, 2009, pp. 1625-1630.
[33] J. Lempert, B. Vadala, K. Arshad-Aliy, J. Roeleveld and A. Emadi, "Practical Considerations for the Implementation of Dynamic Programming for HEV Powertrains," *2018 IEEE Transportation Electrification Conference and Expo (ITEC)*, Long Beach, CA, 2018, pp. 755-760.
[34] X. Zhang, H. Peng and J. Sun, "A Near-Optimal Power Management Strategy for Rapid Component Sizing of Multimode Power Split Hybrid Vehicles," in *IEEE Transactions on Control Systems Technology*, vol. 23, no. 2, pp. 609-618, March 2015.
[35] P.G. Anselma, Y. Huo, J. Roeleveld, G. Belingardi, A. Emadi, "Real-time rule-based near-optimal control strategy for a single-motor multimode hybrid electric vehicle powertrain," *2018 FISITA world congress*, Chennai, India, 2-5 Oct. 208.
[36] S. Yang, W. Wang, F. Zhang, Y. Hu and J. Xi, "Driving-Style-Oriented Adaptive Equivalent Consumption Minimization Strategies for HEVs," in *IEEE Transactions on Vehicular Technology*, vol. 67, no. 10, pp. 9249-9261, Oct. 2018.

Pier Giuseppe Anselma (S'18) received the B.S. and M.S. in mechanical engineering with merits from Politecnico di Torino, Italy, in 2014 and 2017 respectively. He is currently working towards the Ph.D. degree in mechanical engineering at Politecnico di Torino.
In 2016 he was a master's student researcher at the McMaster Institute for Automotive Research and Technology in Hamilton, ON, Canada, where he developed his interest towards the electrification of road vehicles.
His research activities involve design of powertrains and numerical algorithms for optimal control related to electrified and connected vehicles.

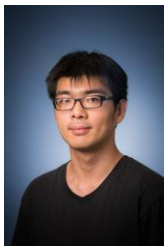

Yi Huo received his B.S. and M.S. in mechanical engineering from Shanghai Jiaotong University (SJTU), China, in 2008 and 2011, respectively. He obtained his Ph.D. degree in mechanical engineering from McMaster University, Canada, in 2018. His research interests include hybrid electric vehicle energy management strategy, engine control, and electrified transmission topology design.

Joel Roeleveld received his B.S. and M.S. degrees in mechanical engineering from McMaster University, ON, Canada, in 2013 and 2015, respectively. He joined the McMaster Automotive Resource Center as a Masters of Applied Science student at McMaster University in September 2013. He is a system modelling and simulation lead for McMaster Formula Hybrid and McMaster Engineering EcoCAR 3 teams in which students compete internationally in design, manufacturing and dynamic competitions. The involvement in these teams along with a design focused undergraduate studies has provoked his to interests in vehicle electrification, focusing on system level simulation, power combination, architecture analysis, and hybrid supervisory control.

Giovanni Belingardi received the M.S. degree in Mechanical Engineering from Politecnico di Torino in 1975.
From 1977 to 1983 he joined the Technical Department of FIAT Auto. Then he came back to Politecnico di Torino and joined the Mechanical Engineering Department as Assistant Professor. Here he developed his academic carrier up to his present position of full Professor.
He is author of more than 280 papers published in international scientific journals and in proceedings of national and international conferences.
He has recently been and at present is the scientific coordinator of the Operative Units of the Mechanical and Aerospace Engineering Department for a number of projects of the framework programs of the European Union, of the National and Regional Governments. Research cooperation with industrial partners has been effective as well.
He is the responsible for International cooperation of Politecnico di Torino within the frame of the Automotive Engineering, with particular attention toward Canada, US, Brazil, Poland and Serbia. Quite frequent visits of those countries give him a special insight of their situation and needs and allowed him to construct a wide net of partnership.

Ali Emadi (S'98–M'00–SM'03–F'13) received the B.S. and M.S. degrees in electrical engineering with highest distinction from Sharif University of Technology, Tehran, Iran, in 1995 and 1997, respectively, and the Ph.D. degree in electrical engineering from Texas A&M University, College Station, TX, USA, in 2000. He is the Canada Excellence Research Chair in Hybrid Powertrain, McMaster University in Hamilton, ON, Canada. Before joining McMaster University, he was the Harris Perlstein Endowed Chair Professor of Engineering and the Director of the Electric Power and Power Electronics Center and Grainger Laboratories, Illinois Institute of Technology (IIT) in Chicago, Illinois, USA, where he established research and teaching facilities as well as courses in power electronics, motor drives, and vehicular power systems. He was the Founder, Chairman, and President of Hybrid Electric Vehicle Technologies, Inc., a university spin-off company of IIT. He is the principal author/coauthor of more than 350 journal and conference papers as well as several books, including Vehicular Electric Power Systems in 2003, Energy Efficient Electric Motors in 2004, Uninterruptible Power Supplies and Active Filters in 2004, Modern Electric, Hybrid Electric, and Fuel Cell Vehicles(2nd ed., 2009), and Integrated Power Electronic Converters and Digital Control in 2009. He is also the Editor of the Handbook of Automotive Power Electronics and Motor Drives in 2005 and Advanced Electric Drive Vehicles in 2014. Dr. Emadi has been the recipient of numerous awards and recognitions. He was the Advisor for the Formula Hybrid Teams at IIT and McMaster University, which received the GM Best Engineered Hybrid System Award at the 2010, 2013, and 2015 competitions. He was the Inaugural General Chair of the 2012 IEEE Transportation Electrification Conference and Expo and has chaired several IEEE and SAE conferences in the areas of vehicle power and propulsion. He is the founding Editor-in-Chief of the IEEE TRANSACTIONS ON TRANSPORTATION ELECTRIFICATION.